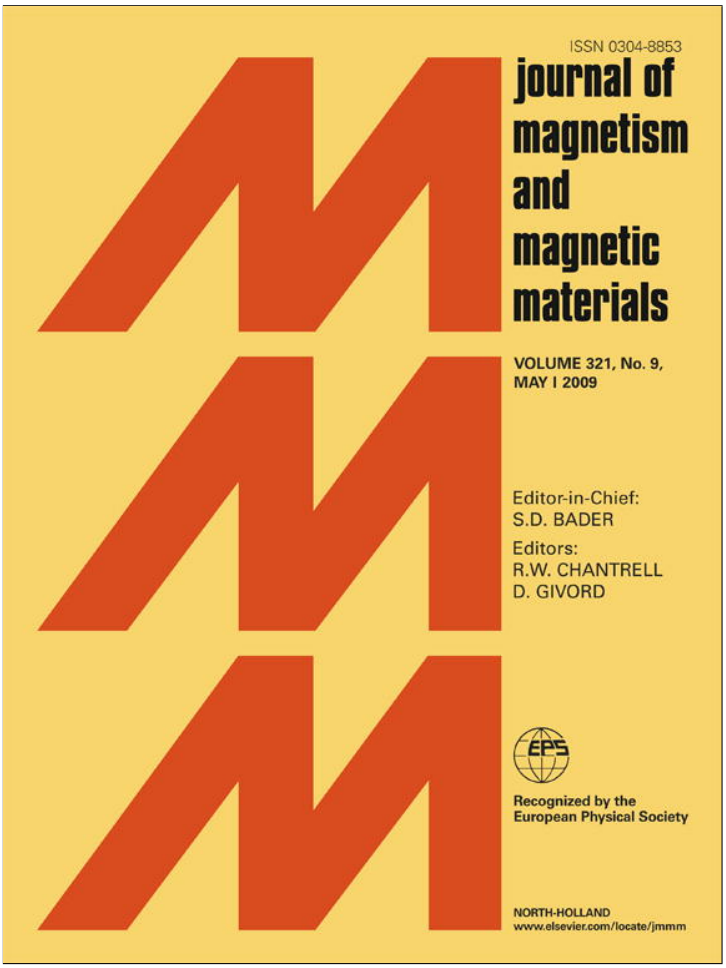

Journal of Magnetism and Magnetic Materials 321 (2009) 1325–1330

Contents lists available at ScienceDirect

Journal of Magnetism and Magnetic Materials

journal homepage: www.elsevier.com/locate/jmmm

Stochastic simulation of thermally assisted magnetization reversal in sub-100 nm dots with perpendicular anisotropy

Budi Purnama *, Masashi Koga, Yukio Nozaki, Kimihide Matsuyama

Kyushu University, Department of Electronics, 744 Motooka Nishi-ku, Fukuoka 819-0395, Japan

ARTICLE INFO

Article history:
Received 4 July 2008
Received in revised form
7 October 2008
Available online 7 December 2008

Keywords:
Thermally assisted magnetization reversal
Reduced barrier writing
Curie point writing
Perpendicular anisotropy

ABSTRACT

Thermally assisted magnetization reversal of sub-100 nm dots with perpendicular anisotropy has been investigated using a micromagnetic Langevin model. The performance of the two different reversal modes of (i) a reduced barrier writing scheme and (ii) a Curie point writing scheme are compared. For the reduced barrier writing scheme, the switching field H_{swt} decreases with an increase in writing temperature but is still larger than that of the Curie point writing scheme. For the Curie point writing scheme, the required threshold field H_{th}, evaluated from 50 simulation results, saturates at a value, which is not simply related to the energy barrier height. The value of H_{th} increases with a decrease in cooling time owing to the dynamic aspects of the magnetic ordering process. Dependence of H_{th} on material parameters and dot sizes has been systematically studied.

1. Introduction

To realize magnetic random access memories (MRAMs) with high bit density of the order of several Gbits/cm^2 and high transfer rates of the order of several Gbits/s, the size of magnetic memory dots should be in the sub-100 nm order and switching time of several nanosecond [1–4]. As a magnetic memory dot is downsized to the sub-100 nm scale, the energy barrier ΔE for magnetization switching tends to become smaller; therefore, a material with high magnetic anisotropy is required. Materials with high perpendicular anisotropy ensure thermal stability that have no scaling limitation in their cell aspect ratio are promising candidate for this purpose. Ultra-thin films having small lateral dot size made of a magnetic material with perpendicular anisotropy can reverse their direction of magnetization through coherent rotation [5], however, the application of a large magnetic field [6] is required for switching. One approach to obtain magnetization reversal in low bias fields is by using the thermally assisted magnetization process [7,8], which implies that the reversal field is temporally reduced by heating of memory cells. In this study, the performance of two different reversal modes of (i) reduced barrier writing and (ii) Curie point writing are compared. Switching fields in the reduced barrier writing scheme are evaluated by considering the energy barrier fluctuation caused by thermal effects. The threshold value of the external field required for aligning the magnetization along the field direction is also evaluated for the Curie point writing scheme.

2. Model

In these micromagnetic simulations, a finite-grid approximation was adopted, where a parallelepiped dot with perpendicular anisotropy was discretized into a two-dimensional array of a rectangular numerical grid. The grid size was chosen to be smaller than the domain wall width. The demagnetization fields are calculated by integrating those from apparent surface magnetic charges on boundary of each grid element [9]. Temporal evolutions of thermally assisted writing processes have been numerically investigated for reduced barrier writing and Curie point writing. For reduced barrier writing, the calculation starts from a uniformly magnetized state at an ambient temperature of 298 K. Simulations of Curie point writing start from just below the Curie temperature T_c, wherein randomly distributed magnetization configurations are used for the initial states. To evaluate the stochastic probability of aligning the magnetization along the field direction, simulations are performed for 50 different random field sequences. An approximation of the thermal fluctuation effect occurring during magnetization is taken into account by involving randomly oriented effective fields with zero mean value, $\langle \mathbf{H}_f^i(t) \rangle = 0$, in the following Landau–Lifshitz–Gilbert (LLG) equation:

$$\frac{d\mathbf{M}^i}{dt} = -|\gamma|\mathbf{M}^i \times \mathbf{H}_{eff}^i + \frac{\alpha}{M_s}\mathbf{M}^i \times \frac{d\mathbf{M}^i}{dt} \quad (1)$$

* Corresponding author. Tel.: +81 92 642 3919; fax: +81 92 642 3971.
E-mail address: b_purnama@spin.ed.kyushu-u.ac.jp (B. Purnama).

0304-8853/$ - see front matter © 2008 Elsevier B.V. All rights reserved.
doi:10.1016/j.jmmm.2008.12.003

The strength of the random field due to the thermal fluctuation effect is calculated by using the fluctuation dissipation theorem [10].

$$\sigma = \sqrt{\frac{2k_B T\alpha}{\gamma V M_s \Delta t}} \tag{2}$$

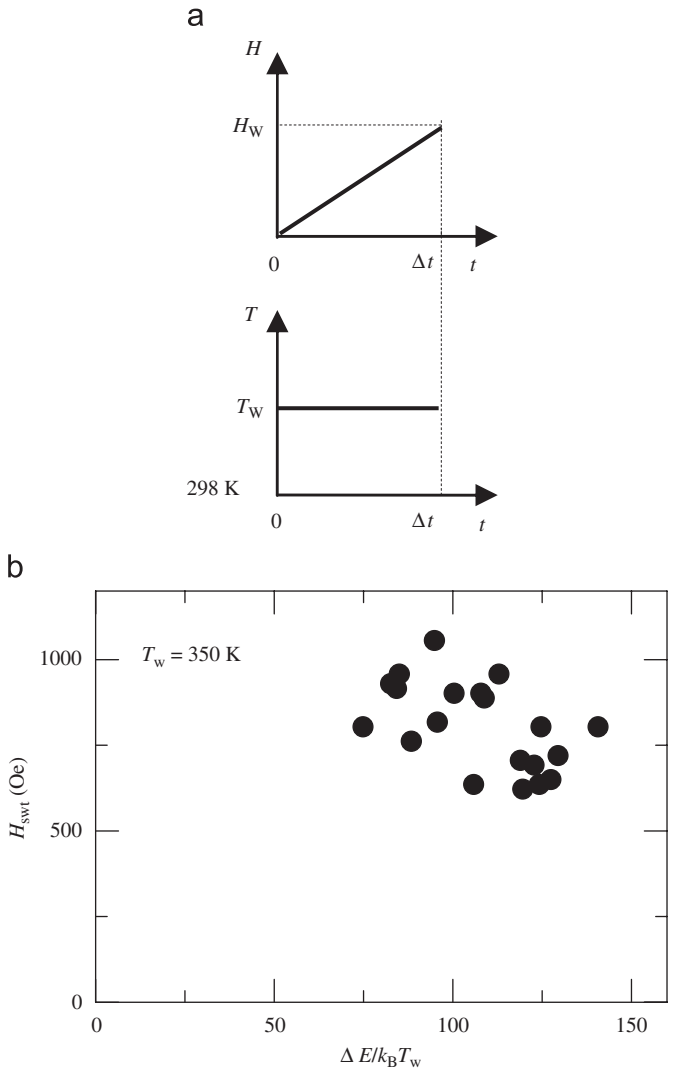

Fig. 1. (a) Simulation model of the reduced barrier writing scheme. (b) Fluctuation of energy barrier ΔE and switching field H_{swt} at $T_w = 350$ K for 20 simulation runs assuming different random field sequences.

where α is the Gilbert damping constant ($= 0.3$), $\gamma = 1.76 \times 10^7$ ($Oe^{-1}\,s^{-1}$) is the Gyromagnetic ratio, V is the volume of the subcell and the time step of the integration time methods, dt is 0.25 ps. In our model, an amorphous ferrimagnetic material is considered as a composition of magnetic nanocells, so that the second-power temperature dependence with the thermally reduced magnetization was assumed for both the exchange stiffness constant, A, and the perpendicular crystalline anisotropy, $K_\perp$ [11]: $A(T) = A^{(0)}(M_s(T)/M_s(0))^2$, $K_\perp(T) = K_\perp^{(0)}(M_s(T)/M_s(0))^2$. A simple empirical temperature dependence of the magnetization, $M_s(T) = M_s^{(0)}(1-T/T_c)^{0.5}$, is adopted, which reasonably fits the experimental result. Other material parameters used in the simulation are as follows: $A = 1.0 \times 10^{-7}$ erg/cm (at 298 K) [12], $T_c = 373$ K. Any spatial disorder is not assumed for the magnetic parameters including M_s, A, $K_\perp$ and the easy axis direction. In most of the following simulations, the grid size of 3.3 nm was used, M_s and $K_\perp$ values are set such that the energy barrier height $\Delta E \geqslant 60k_BT_a$ (T_a is an ambient temperature of 298 K) to ensure that practical thermal stability is achieved.

3. Results and discussions

Fig. 1(a) illustrates the simulation model of the reduced barrier writing scheme. In this model, the uniformly magnetized state is set as the initial condition. The uniform reversal field is then linearly increased with the increasing time periods Δt at a fixed temperature T_w. The value of Δt and the final external field are chosen to be 2.5 ns and 1400 Oe, respectively. The resultant field ramp rate is 560 Oe/ns. Fig. 1(b) shows the typical stochastic switching properties due to variation in the thermal fluctuation effects of 20 random field sequences at $T_w = 350$ K.

Simulations were performed for a nanodot of $50 \times 50 \times 20\,nm^3$ volume having the following magnetic properties: $K_\perp = 8.8 \times 10^4$ erg/cm^3 and $4\pi M_s = 1.9$ kG. The switching field H_{swt} is defined as a field value at which the average magnetization becomes zero during the magnetization reversal process. The energy barrier ΔE between the bi-stable magnetization states is also evaluated from the magnetization reversal simulation, which is defined as a deference between the maximum and the minimum value of the total magnetic energy during the magnetization reversal, including the exchange, demagnetizing and anisotropy energy terms. A particular thermal fluctuation sequence corresponds to a particular type of the energy barrier ΔE, thus reflecting the random aspects. Therefore, the field required for switching H_{swt} in the reduced barrier writing scheme strongly depends on the variation in the micromagnetic configuration caused by the thermal effects modelled by the random field. In a simple coherent rotation model, the switching field simply depends on the energy barrier

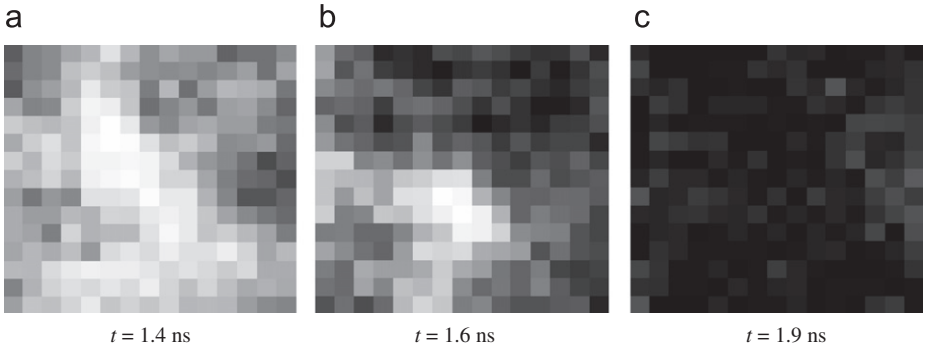

Fig. 2. Micromagnetic configurations in the reduced barrier writing scheme: (a) domain nucleation, (b) domain expansion and (c) domain annihilation. The grey scale denotes the magnetization along the field direction; with black being full scale in one direction, whereas white in the other.

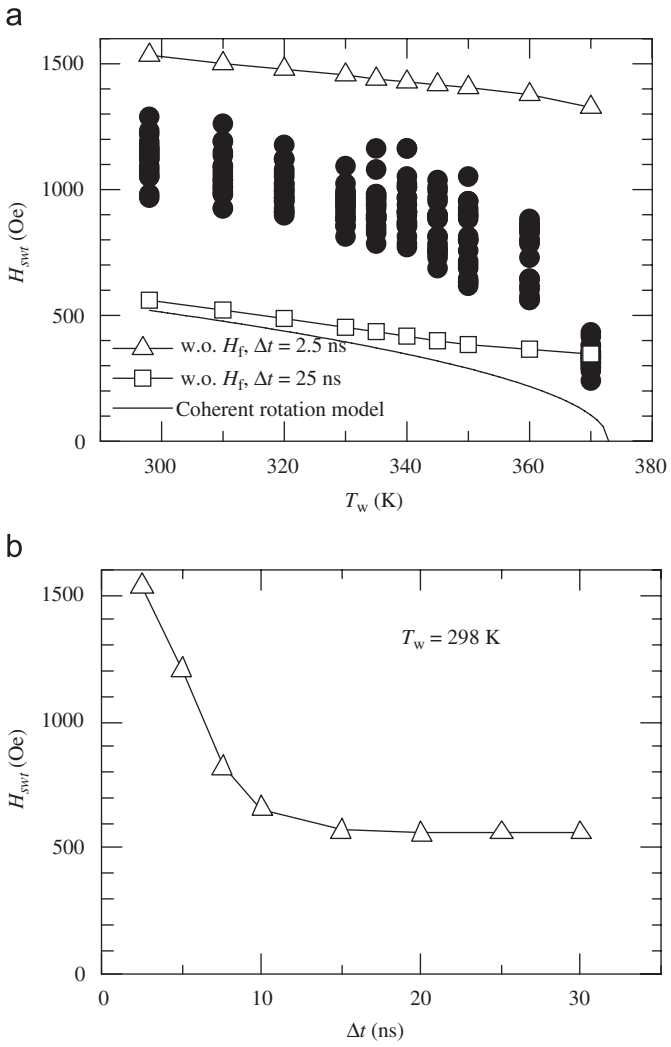

Fig. 3. (a) Dependence of switching field H_{swt} on temperature computed for different simulation models. (b) Dependence of H_{swt} on increasing Δt of the external field.

height. However, we observed that H_{swt} takes different values. This may be because local pinning effects dominate H_{swt}, which is not related to the averaged ΔE due to the stochastic aspect in the thermally assisted magnetization switching. Fig. 2 shows typical micromagnetic configurations of non-uniform magnetization reversal during the reduced barrier writing at 350 K for the dot shown in Fig. 1(b). The magnetization switching started from domain nucleation (a) then domain expansion (b) and domain annihilation.

Considering the stochastic aspect of the reduced barrier writing scheme, simulations are performed using 20 different random field sequences at each temperature, as shown in Fig. 3(a). The significant scattering of H_{swt} can be attributed to the variation in an individual random field series. In comparison, simulations are also performed without random fields for $\Delta t = 2.5$ and 25 ns, by considering only the temperature dependence of material parameters. As demonstrated in the figure, the thermal fluctuation, modelled by random fields, effectively assists the switching events and leads to a considerable reduction in H_{swt}, it also

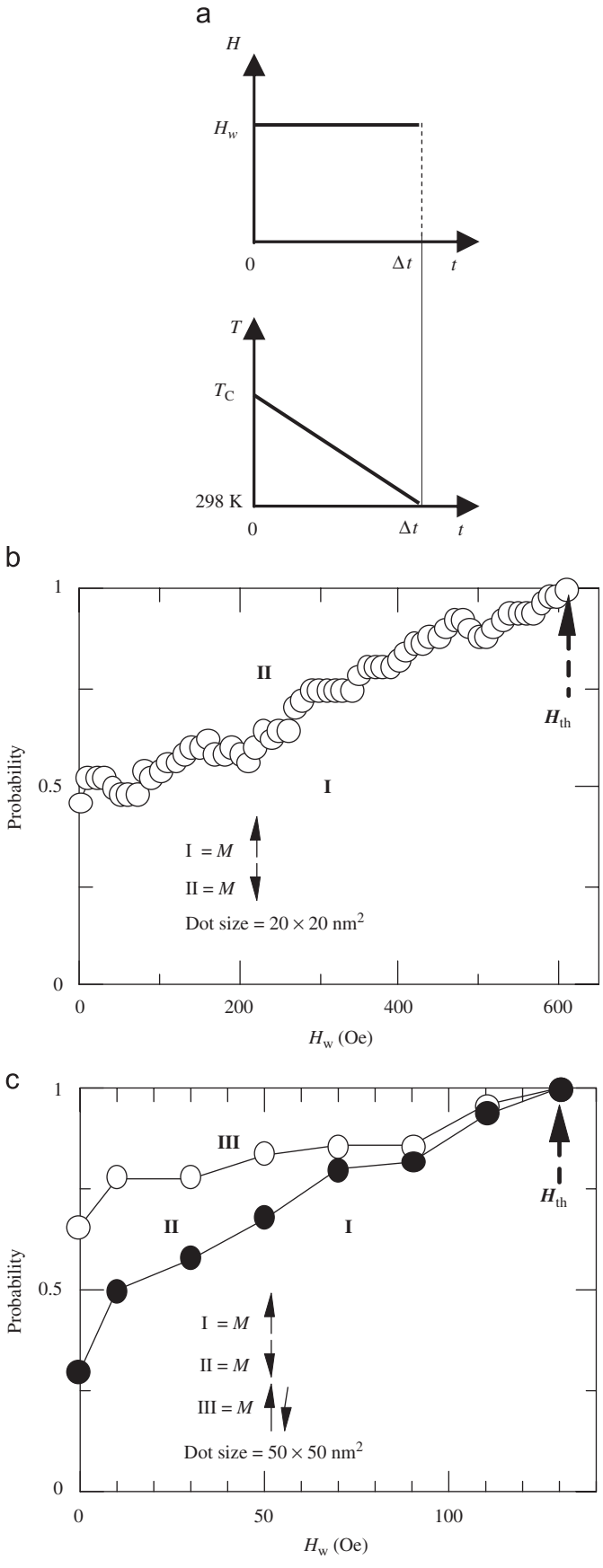

Fig. 4. (a) Simulation model of Curie point writing scheme. The probability of final magnetization states occurring after writing for dots with different sizes and material parameters: (b) $20 \times 20 \times 20\,nm^3$, $K_\perp = 2.93 \times 10^5\,erg/cm^3$ and $4\pi M_s = 1.88$ kG, (c) $50 \times 50 \times 20\,nm^3$, $K_\perp = 8.73 \times 10^4\,erg/cm^3$ and $4\pi M_s = 1.88$ kG. Δt of 2.5 ns was used in this simulation.

introduces a dispersion of H_{swt} values. The significant difference in H_{swt} for reference simulations with $\Delta t = 2.5$ and 25 ns can be explained in terms of the dynamic coercivity. Fig. 3(b) shows H_{swt} evaluated for various Δt at 298 K, where random fields are not taken into account. The value of H_{swt} decreases with an increase in Δt and reaches a minimum value of 600 Oe at $\Delta t = 15$ ns, where the switching behaviour becomes quasi-static. The quasi-static switching field at 298 K is reasonably consistent with a simple theoretical prediction based on the coherent rotation model. The demagnetization coefficient of the simulated dot ($50 \times 50 \times 20$ nm^3) along the perpendicular axis is estimated at 0.57. The simulated values of H_{swt} (open square symbols in Fig. 3(a)) deviate from the coherent rotation model with the increase in temperature. This can be reasoned that the domain nucleation mode dominates the magnetization switching of the dot with the thermally reduced exchange stiffness, as demonstrated in Fig. 2. Pinning of the temporal domain state would cause higher H_{swt} in the high temperature region.

Fig. 4(a) illustrates the simulation model of the Curie point writing scheme. A uniform external field H_w is applied along the perpendicular anisotropy axis, while the temperature is linearly lowered from the Curie temperature T_c (373 K) to ambient temperature (298 K). This means that a magnetic ordering process is involved in this writing scheme. Although the actual temperature decay should be exponential, it was confirmed that the fundamental properties are obtained with reasonable accuracy by a linear decay approximation. This is because magnetic ordering dominates at an early stage in the cooling process. Fig. 4(b) and (c) shows the probability of final magnetization states occurring after the writing process. The probability was evaluated at each value of H_w from 50 simulation results by assuming different initial magnetization states and random fields. In the simulation, the aligning event is considered to occur when M_{easy}/M_s exceeds 0.85 [13]. A definition of the threshold field H_{th} required for aligning the magnetization along the field direction is presented in Fig. 4(b) and (c). That is, H_{th} presents a criterion at which the successful writing was performed in all of the 50 simulation results. Simulations were performed for two dots with different sizes and material parameters as follows: (1) $20 \times 20 \times 20$ nm^3 and $K_\perp = 2.93 \times 10^5$ erg/cm^3, $4\pi M_s = 1.88$ kG (referred to as dot A hereafter); (2) $50 \times 50 \times 20$ nm^3, $K_\perp = 8.73 \times 10^4$ erg/cm^3, $4\pi M_s = 1.88$ kG (dot B). Δt of 2.5 ns was used in this simulation.

Fig. 4(b) shows that when the field is equal to zero, dot A relaxed into single domain up ($M\uparrow$: along H_w, noted as region 1 in the figure) or single domain down ($M\downarrow$: opposite to H_w, region 2) with the same probability of 0.5. In the case of dot A, the multi-domain configuration was not observed for the 50 simulations. By increasing the external field, the probability of $M\uparrow$ increases and becomes equal to 1 at $H = H_{th}$. Fig. 4(c) presents the results for dot B. For zero fields cooling, three types of magnetization reversal appear: single domain up ($M\uparrow$), single domain down ($M\downarrow$) and the multi-domain configuration ($M\uparrow\downarrow$). For the Curie point writing scheme, it is predicted that the threshold field not only depends on the physical properties associated with the material parameters, but is also affected by the stochastic magnetic ordering process.

A micromagnetic ordering process in the Curie point writing is shown in Fig. 5. The initial state of randomly oriented magnetization configuration rapidly relaxes to the single domain configuration, taking the transient multi-domain configuration (Fig. 5(b)).

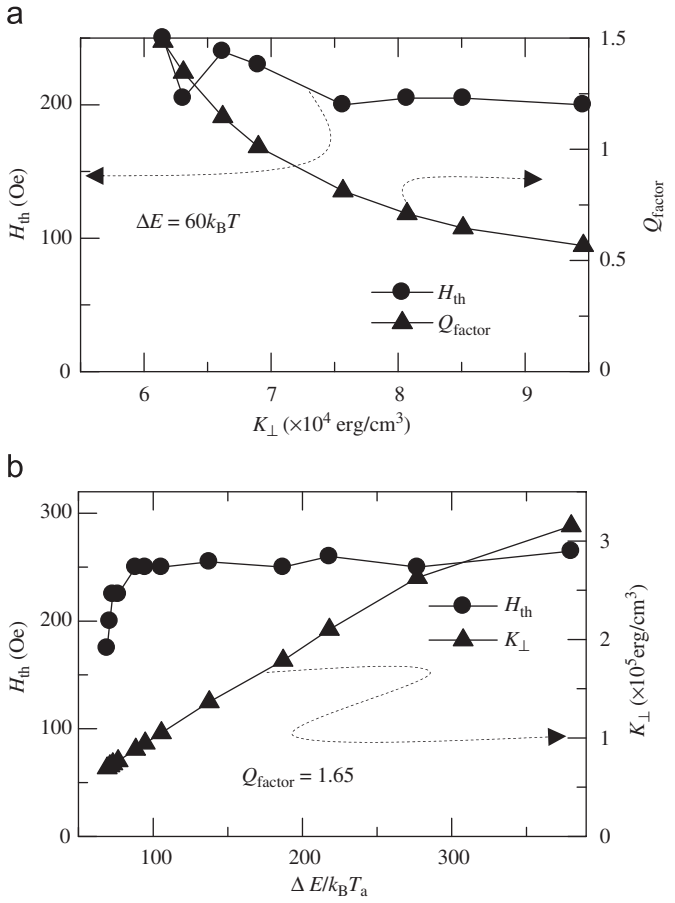

Fig. 6. (a) Threshold field H_{th}, required for aligning the magnetization along the field direction as a function of perpendicular anisotropy $K_\perp$ for a fixed energy barrier ΔE of $60k_BT_a$ ($T_a = 298$ K). (b) Dependence of H_{th} on ΔE for a fixed Q_{factor} of 1.65. Both for (a) and (b) calculated for Δt of 2.5 ns and dot size of $50 \times 50 \times 20$ nm^3.

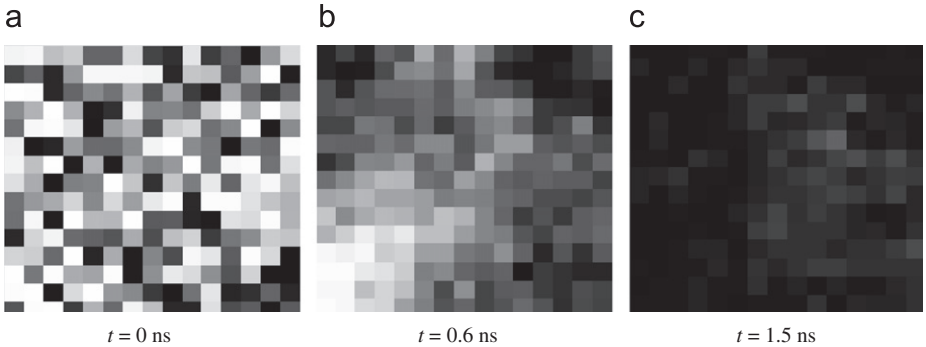

Fig. 5. Micromagnetic ordering process in the Curie point writing scheme. (a) initial random state, (b) local ordering of domain configuration and (c) final single domain configuration. The grey scale denotes the magnetization along the field direction; with black being full scale in one direction, and white the other.

Fig. 6(a) shows H_{th} as a function of $K_\perp$ for dot B, where M_s is chosen such that ΔE is constant at $60k_BT_a$. Since the energy barrier ΔE is related to the perpendicular anisotropy term and the demagnetizing one, the values of an additional parameter of Q_{factor} ($=K_\perp/2\pi M_s^2$) are also presented in the figure. The results demonstrate that the values of H_{th} slightly fluctuate for lower $K_\perp$, but are mostly constant at 200 Oe, although values of Q_{factor} are significantly different. Another aspect of H_{th} on the material parameters is also demonstrated in Fig. 6(b). Here, Q_{factor} is fixed at a 1.65 and ΔE is varied by varying $K_\perp$ and $4\pi M_s$. In this case, H_{th} increases with an increase in ΔE and saturates at 250 Oe, for ΔE greater than $90k_BT_a$.

Fig. 7(a) shows occurrence probability of aligning the magnetization along the applied field direction for various values of H_w at various cooling times Δt. The simulations are performed for dot B ($20\times20\times20\,nm^3$, $K_\perp=2.93\times105\,erg/cm^3$, $4\pi M_s=1.88$ kG and $\Delta t=2.5$ ns). The probability increases with the increase in Δt for each value of H_w, reflecting the dynamic aspect in the magnetization ordering process. Under zero field writing $H_w=0$, the significant degradation in probability for smaller Δt is mainly because the magnetization state freezes at a local minimum state of the multi-domain configuration. It should be noted that the multi-domain state does not occur for Δt larger than 2.5 ns. As a result, with zero fields cooling, the probability is about 0.5, for either the single domain up or the single domain down magnetization.

The threshold field H_{th}, at which the probability becomes 1, decreases with the increase in Δt and reaches a saturation value of 100 Oe at 2.5 ns. The transient time is markedly shorter than that for the reduced barrier writing scheme (about 15 ns), as shown in Fig. 3(a).

Fig. 8 shows the dependence of the Curie point writing property on the dot size. In this simulation, the saturation induction $4\pi M_S$ is fixed at 1.88 kG, while the value of the perpendicular anisotropy $K_\perp$ is chosen such that the energy barrier ΔE becomes constant at $60k_BT_a$ for individual dot sizes ranging from $20\times20\times20$ to $80\times80\times20\,nm^3$. Fig. 8(a) plots the probability of aligning along the field direction as a function of the writing field H_w, with the dot size as a parameter.

As also discussed in the previous paragraph, the size dependence of the Curie point writing property can be related to the domain wall width. The wall width $\delta_w(=\pi(A/K_\perp)^{1/2})$ of the 20 nm dot is 18 nm, which is almost the same as its lateral

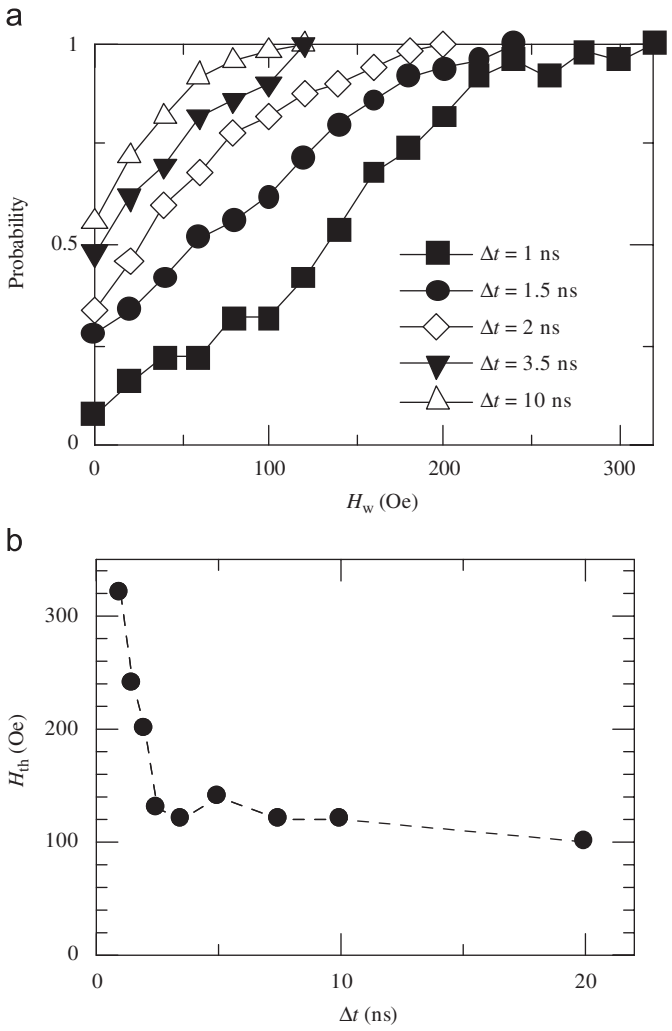

Fig. 7. (a) Probability of aligning the magnetization along the field direction as a function of external field for different cooling times Δt in dot size of $50\times50\times20$ nm^3. (b) Threshold field H_{th} vs. Δt.

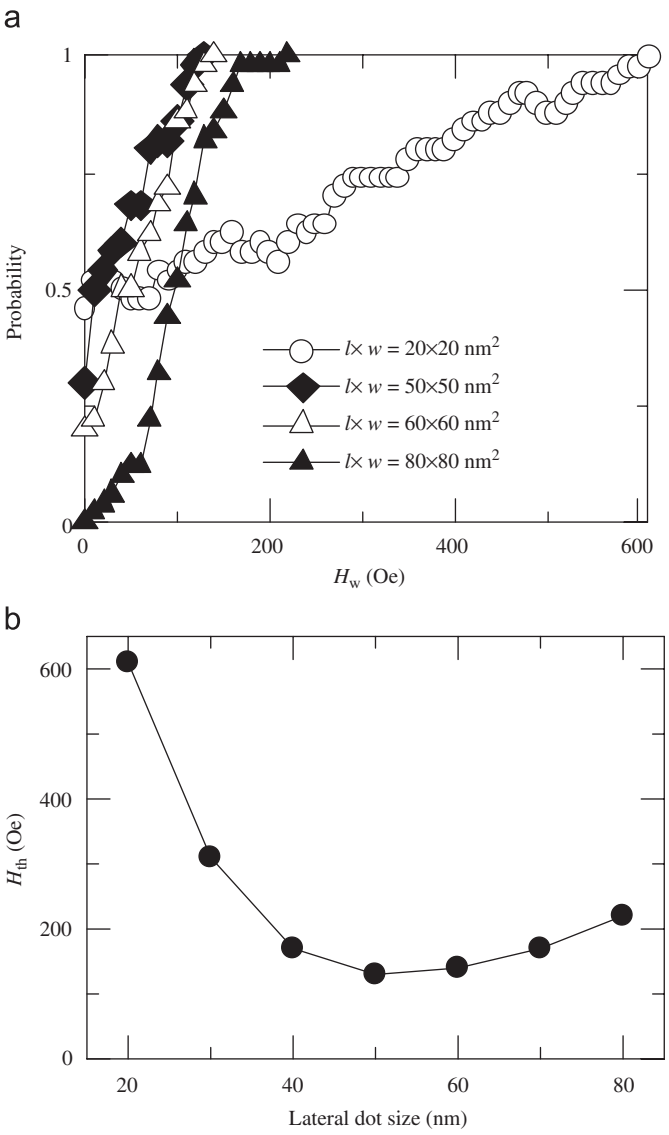

Fig. 8. (a) Probability of aligning the magnetization along the field direction as a function of external field for various dots calculated in Δt of 2.5 ns. (b) Threshold field H_{th}, required for successful Curie point writing, evaluated for various dots with different sizes but having the same energy barrier height between the bi-stable states.

dimension. On the other hand, δ_w of the 80 nm dot is 36 nm, which is much smaller than the dot size. Consequently, the temporal local magnetic ordering formed in the cooling process is likely to be relaxed to a multi-domain configuration in the larger dot, whereas it disappears in the smaller dot.

Fig. 8(b) shows the threshold field H_{th} as a function of the dot size. H_{th} reaches a minimum of 130 Oe for a dot size of 50 nm. The increase in H_{th} for the smaller dots can be related to the larger $K_\perp$ assumed to satisfy the energy barrier limit of $60k_BT_a$. Consequently, it can be deduced that H_{th} is dominated by the anisotropy energy for the single domain dots. In addition, the increase of H_{th} for the larger dots can be associated with complicated local ordering and its elimination process.

4. Summary

In summary, we have numerically investigated the thermally assisted writing of different modes of (i) a reduced barrier writing scheme and (ii) a Curie point writing scheme. In this study, we focus on sub-100 nm dots with perpendicular anisotropy $K_\perp$. Though the switching field in the reduced barrier writing scheme decreases with an increase in temperature, it is still higher than that in the Curie point writing scheme. The threshold field H_{th} required to define the magnetization direction in Curie point writing was evaluated for dots of various sizes and material parameters. The value of H_{th} increases with the increase in $K_\perp$ for the single domain dot. Multi-domain configuration in the larger dots is another reason for the increase of H_{th}. When the cooling time in Curie point writing is shorter than a critical value, H_{th} significantly increases.

Thermally assisted MRAM is one promising technology in the next memory generation as it can solve both the problems of write selectivity and thermal stability while scaling down to below 100 nm dots order. An additional mechanism such as lowering E_b by interlayer exchange field in a magnetic bi-layer system may improve memory performance.

Reference

[1] S.E. Russek, R.D. McMichael, M.J. Donahue, S. Kaka, Top. Appl. Phys. 87 (2003) 93.
[2] Y. Nozaki, K. Matsuyama, J. Appl. Phys. 93 (2003) 7295.
[3] T. Devolver, C. Chappert, J. Appl. Phys. 95 (2004) 1933.
[4] R.H. Koch, G. Grinstein, G.A. Keefe, Y. Lu, P.L. Trouilloud, W.J. Galangher, S.S.P. Parkin, Phys. Rev. Lett. 84 (2000) 5419.
[5] R. Skomsi, H.-P. Oepen, J. Kirschner, Phys. Rev. B 58 (1998-) 3223.
[6] H. Meng, J.-P. Wang, Appl. Phys. Lett. 88 (2006) 172506.
[7] M. Kerekes, R.S. Sousa, I.L. Prejbeanu, O. Redon, U. Ebels, C. Baraduc, B. Dieny, J.-P. Nozieres, P.P. Freitas, P. Xavier, J. Appl. Phys. 97 (2005) 10P501.
[8] J.P. Attane, D. Ravelosona, A. Marty, Y. Samson, C. Chappert, Phys. Rev. Lett. 96 (2006) 147204.
[9] C.C. Shir, J. Appl. Phys. 49 (1978) 3413.
[10] W.F. Brown Jr., Phys. Rev. 130 (1963) 1677.
[11] M. Mansuripur, G.A.N. Connel, J. Appl. Phys. 55 (1984) 3049.
[12] M. Mansuripur, J. Appl. Phys. 63 (1988) 5809.
[13] B. Purnama, Y. Nozaki, K. Matsuyama, J. Magn. Magn. Mater. 310 (2007) 2683.